

A Physical Model of the Electron According to the Basic Structures of Matter Hypothesis *

Dr. Stoyan Sarg

Abstract: A physical model of the electron is suggested according to the Basic Structures of Matter (BSM) hypothesis (later published as a BSM-SG theory). BSM-SG is based on an alternative concept about the physical vacuum assuming that the space contains underlying superfine structure of nodes formed of super-dens sub-elementary particles, which are also involved in the structure of the elementary particles. The proposed grid structure is formed of vibrating nodes possessing quantum features and energy well. It is admitted that this hypothetical structure could be accounted for the missing “dark matter” in the Universe. The signature of such “dark matter” is apparent in the galactic rotational curves and in the relation between masses of the supermassive black hole in the galactic centre and the host galaxy. The suggested model of the electron possesses oscillation features with anomalous magnetic moment and embedded signatures of the Compton wavelength and the fine structure constant. The analysis of the interactions between the oscillating electron and the nodes of the vacuum grid structure allows obtaining physical meaning for some fundamental constants.

Keywords: physical vacuum, structure of the electron, fine structure constant, Compton wavelength, anomalous magnetic moment, dark matter, Planck frequency, unified theories

1. Introduction

The “dark matter” is a hot topic in the cosmology today. Currently it is accepted that the “dark matter” predominates the visible matter in the Universe. In recent years it has been found that most of galaxies contain in their centre a supermassive black hole in order of billion solar masses. A surprising strong relation has been found between the mass of the supermassive black hole and the total mass of the whole galaxy, so they are in kind of balance¹ (L. Ferrarese, D. Merrit, 2000). Another peculiar fact for existence of hidden matter comes from the rotational curves of the galaxies. One of the largest rotation curve data base of spiral galaxies clearly shows that the “dark matter” is rather a rule, than exception (see the article “An analysis of 900 optical rotation curves: Dark matter in a corner?”, by D. F. Roscoe, (1999)²). It stands to reason raising a question: Isn’t the “dark” matter a hidden type of matter around us and even “within us”? Such idea further leads to the conclusion that the currently adopted concept about the physical vacuum may not be correct. This required an extensive study of some features of the physical vacuum such as the Zero Point Energy, the quantum fluctuations, the vacuum polarization, the Planck’s length and frequency and so on. In such aspect, the theoretical articles provided by T. H. Boyer³, H. E. Puthoff^{4,5,6}, H. E. Puthoff et al⁷, B. Haisch et al.⁸ appeared quite useful. F. M. Meno⁹ envisions hypothetical three-dimensional non-spherical particles called gyrons possessing a gyroscopic effect. He associate the Planck’s length and mass to some of the gyron’s parameters, although he does not suggest a detailed physical model of this gyron and does not envision a possible organization of the gyrons into stable structures. The articles “Experimental evidence that the gravitational constant varies with the orientation” by M. M. Gershteyn et al¹⁰ and the “Speed of gravity revisited” by M. Ibison et al¹¹ lead to the idea that the Newton’s law of gravitation might be derivable instead of postulated. This idea obtained some theoretical treatment by H. E. Puthoff⁴ (1989) who derived the Newton’s law of gravitation starting from the Planck’s frequency, ω_{PL} , and using one hypothesis of Sakharov.

$$\omega_{PL} = [2\pi c^5 / hG]^{1/2} \quad (1)$$

where: c – is the light velocity, h – is the Planck constant, G – is the gravitational constant

Here we may express an idea about existence of some hypothetical structure in the microscale range, related in some way to ω_{PL} . This could be regarded as a further development of the concept of the string theories which assume an existence of some hypothetical string-like objects (open or closed loops) in a microscale range possessing a finite length but zero thickness. What could be the results if these hypothetical extended objects possessed a finite width, while their dimensions are far beyond the observational limit. In such case these strings

should be regarded as material objects in a three-dimensional space and they might be organized in structures. It stands to reason that we are able to observe enormously large structures in the macroscale range of the Universe, but structures may exist also in the microscale range¹².

One additional consideration that the Newton's law of gravitation might be derivable from a more fundamental one comes from its comparison with the law of optical radiation. In its simplest form, when the surface of two areas A_1 and A_2 are parallel each other, the irradiation flux, Φ , is given by: $\Phi = LA_1A_2/r^2$ where L – is the emitted radiance and r – is the distance between the two surfaces (visible in the subtended angle). If the two bodies are parallel disks, the radiation law depends only on the visible surfaces but not on the disk thickness. In the same time the Newton's gravitational law depends on the thickness or the bulk matter of the bodies. But why they both have one and a same dependence on the distance? It seems that the Newton's gravitational mass could have some dependence on the area of the closed surface of some unknown real structure on which some hypothetical substance may exercise pressure.

The above-mentioned citations and logical considerations were helpful in the search for appropriate model of the alternative vacuum concept. An idea was born that the Planck's frequency could be a parameter of some intrinsic type of matter involved in some unknown sub-elementary particles from which both - the vacuum structure and the elementary particles are built. These hypothetical sub-elementary particles may possess enormous mass density and may interact between themselves in a classical void space. Their gravitational interactions, however, may distinguish from the Newton's gravitation by the degree of proportionality to the distance. In such aspect, we may refer such type of gravitational interactions as Super Gravitation (SG). The hypothetical sub-elementary particles, for instance, may form stable structures if their SG forces in a classical void space is inverse proportional to the cube of the distance. In such way they may form a stable spatial grid. *At the same time the Newton's gravitation acting between the elementary particles and their formations (atomic nuclei, atoms, molecules) could be a result of the SG field propagation through the interconnected elements of the spatial grid.* The SG field, however, may leak at some close distance between atoms and molecules (some types of Wan der Waals forces) or well polished solid objects (Casimir forces).

2. Brief introduction into the concept of BSM hypothesis

The presented above considerations served as a starting point for development of a hypothesis called Basic Structures of Matter (BSM)¹³, associated to the class of the unified theories. According to the BSM concept¹⁴ the Super Gravitation (SG) force, F_{IG} , between two objects comprised of same type of intrinsic matter put in a classical void space is proportional to the product of their intrinsic masses and the Super gravitational constant and inverse proportional to the cube of the distance.

$$F_{IG} = G_0 \frac{m_{01}m_{02}}{r^3} \quad (2)$$

where: G_0 – is the SG constant, m_{01} and m_{02} – are intrinsic masses, r – is the distance.

It is assumed that the space known as a physical vacuum possesses a underlying grid structure formed of two types of sub-elementary particles arranged in nodes. These two sub-elementary particles are built respectively by two types of intrinsic matter with different density. They both have a shape of hexagonal prisms with length to diameter ration > 1 , while the dimensional ratio between both prisms is 2:3. They possess also a similar internal structure with twisted component, but left and right handed respectively. Prisms of the same type (intrinsic matter and handedness) are attracted in a pure void space by forces according to defined above SG law. The attraction forces between the different types of prisms, however, are smaller and dependable on the node distance and they may convert to repulsion at some critical value of this distance. Additionally the prisms of both types possess SG anisotropy along their axis with a left and right twisting component respectively, defined by their lower level structure. For this reason they are called twisted prisms, although, they are not externally twisted. The formation of such sub-elementary particles is possible from much simpler spherical particles, following pure geometrical principles and preservation of the integrity of the lower level structures in the upper level structures. A hypothetical scenario for this is provided in Chapter 12 of BSM. According to the BSM concept, the two types of prisms build the underlying structure of the physical vacuum and the elementary particles as well. The structural integrity in both cases is assured by the SG law, defined by Eq. (2). The elementary component of the vacuum structure is a node called a Cosmic Lattice (CL) node. The CL node is formed of four prisms of a same type held

by SG forces in positions like the four axes in a tetrahedron, but the connected prisms have some limited freedom of angular deviation. The vacuum structure is formed by alternatively arranged nodes of both types with some gaps between the prisms of the neighboring nodes. The spatial CL structure is similar to the atomic lattice in a diamond. It is assumed that such structure fills the volume of the visible Universe, so the space in BSM is referenced as a CL space. The elementary particles are built by the same prisms, but arranged in configuration of helical structures inside of which a different type of spatial structure (internal lattice) from the same prisms exists. The internal lattice, however, is denser than the CL structure, so the latter could not penetrate inside the internal lattice. Therefore, the CL space should exercise a pressure on the internal lattice of the particle. The pressure parameter of the CL space leads to derivation of a mass equation in BSM (Chapter 3). It is estimated that the node distance is in order of 10^{-20} (m), while the overall size of any elementary particle is larger by few orders. In the same time the density of the intrinsic matter from which the prisms are built is many orders larger than the average density of any elementary particles. In such conditions the CL space is able to carry the elementary particles, while an accumulation of these particles in a closed volume may influence but very weakly the node distance of the CL space in a close proximity (a large mass accumulation may distort slightly the node distance in the surrounding space leading to a space curvature according to the General Relativity).

One specific feature of the CL space is the ability of the CL nodes to be displaced by the denser internal lattice of the moving elementary particles (every particle is in motion due to the galactic rotation). Such effect involves a disconnection, a displacement with simultaneously folding of the CL node and returning, unfolding and reconnection to the previous position of CL structure. The connection energy during the displacement is transferred to a kinetic energy. Such unique feature does not have counterpart in any concept of aether or ideal fluid. The folding properties of the CL nodes are also closely related to the inertial properties of the atomic matter in CL space and play a role in the equivalence between the gravitational and inertial mass.

Analysing the dynamics and mutual interactions of the CL nodes, it is possible to associate some of their features with known physical parameters and constants such as, the Zero Point Energy of the vacuum, the light velocity, the Compton frequency (or wavelength), the permeability and permittivity of the free space. Figure 1 illustrates the geometry of a single CL node in a position of geometrical equilibrium. The four prisms are held by SG forces defined by Eq. (2).

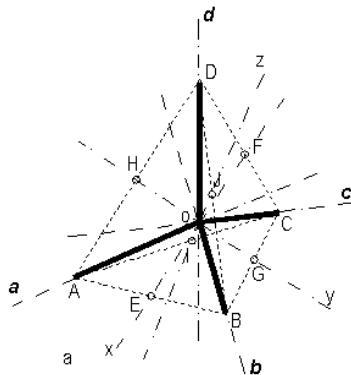


Fig. 1. CL node formed of four prisms shown by thick black lines

The CL node is characterized by two sets of axes: one set of 4 axes along anyone of the prisms called *abcd* axes, and another set of 3 orthogonal axes called *xyz* axes. In a geometrical equilibrium the angle between anyone of *abcd* axes is 109.5° . The external tips of the prisms in a geometrical equilibrium define the apex points of a tetrahedron. The *xyz* axes pass through the middle of every two opposite edges of the tetrahedron. In the same time, the orthogonal *xyz* axes of the neighbouring CL nodes are commonly aligned. Such arrangement assures complex individual oscillations of the CL node, from one side and strong interactions between the neighbouring nodes, from the other. The dynamics and interactions are both governed by the SG law acting between the two intrinsic matter substances of the prisms and the time constant for this matter.

The dynamical behaviour of the CL node is studied by estimating the shape of the return forces (under condition of SG law) acting on the deviated from the central position CL node and keeping in mind that the node geometry is flexible. For simplification of the analysis, the neighbouring four CL nodes are considered stationary, while their interconnecting prisms are always aligned to the CL node under consideration (for details see BSM

monograph, BSM_appendix2-1.pdf). This also means, that the SG interactions propagate faster than the oscillation period of the CL node. The shapes of the return forces along anyone of xyz and $abcd$ axes are shown respectively in Fig 2. (a) and (b).

Two symmetrical minimums appear along anyone of xyz axes and one minimum along the positive direction of anyone of $abcd$ axes. From a point of view of CL node dynamics, they could be associated with energy wells, responsible for the ZPE (zero point energy) of the vacuum.

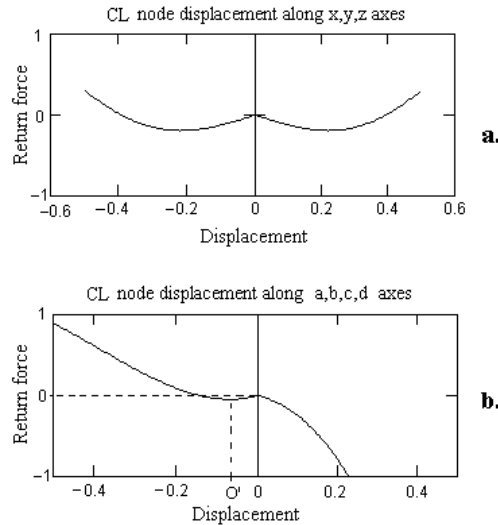


Fig. 2. Return forces versus displacement of the CL node along one of xyz axes (a) and $abcd$ axes (b). Both scales are in relative units.

The shape and the different stiffness of the return forces along xyz and $abcd$ axes indicates that the CL node will possess a complex type of oscillations in which two types of cycles are identifiable: a proper resonance cycle and a SPM cycle (the latter is described by a Spatial Precession Momentum vector). The trace of the proper resonance cycle is approximately flat but open curve with four bumps, as shown in Fig. 3.

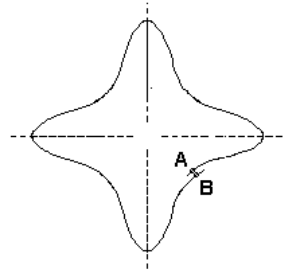


Fig. 3. Trace of single proper resonance cycle of the CL node

The bumps of the trace curve centred on the two orthogonal axes are caused by the different stiffness for node deviations along $abcd$ and xyz axes. The points A and B from the resonance cycle are pretty close but not coinciding, so the segment AB points almost at 90 deg in respect to the drawing plane. The lack of coincidence between any initial (A) and final (B) point for one proper resonance cycle is a result of the spatial positions of the return forces minimums along the two set of axes. The CL node dynamics for the proper resonance cycle could be described by a vector called a Node Resonance Momentum (NRM).

The average plane of the trace is slightly rotating with every NRM cycle, so after a large number of such cycles the node trace will pass through the same (arbitrary selected) initial point A. This second type of cycle is called a SPM cycle. The vector describing this cycle is called a Spatial Precession Momentum vector (SPM). The number of the resonance cycles in one SPM cycle, estimated in BSM, is quite large but constant (due to the mutual interactions of the oscillating CL nodes). The analysis in BSM indicates that this number is related to the magnetic permeability of free space (section 2.11.3 in chapter 2 of BSM).

The tip of SPM vector for one full cycle circumscribes a closed surface with a central point of symmetry and six bumps along the axes xyz . Such type of surface is referenced in BSM as a SPM quasisphere. It is found that if the resonance cycle of the CL node is related to the energy wave propagation with a light velocity, the SPM cycle should be related to a particular quantum feature of the CL space that assures the constant value of the light velocity. This is explainable by the quantum properties of the SPM quasispheres and their mutual interactions. The light velocity is considered as energy momentum propagation between two neighbouring nodes (considering xyz interconnection coordinates) for one resonance cycle of the CL node (section 2.11 in Chapter 2 of BSM). The frequency of SPM cycle is associated to the well-known Compton frequency. In absence of any electrical charge, the SPM quasisphere possesses a central point of symmetry. It is called a Magnetic Quasisphere (MQ), because it could provide a physical meaning of the magnetic line. The magnetic line could be formulated as **a closed loop in CL space involving only MQ type of nodes whose SPM frequencies are synchronized by a running phase propagating with a light velocity**. Such spatial configuration may exhibit features allowing explanation of the stability and direction of the magnetic line, for example:

- The CL nodes of right-handed prisms are commonly synchronized
- The CL nodes of the left-handed prisms are commonly synchronized
- The phase difference between the involved left and right handed nodes determines the direction of the magnetic line, referenced to the laboratory frame, for example, +90 deg phase difference for N-S direction and -90 deg phase difference for S-N direction.
- The involved MQ nodes may additionally have a helical arrangement along the closed loop.

The above considerations are for permanent magnetic field. In case of alternative magnetic field, the commonly spatially dependable synchronizations of the left and right-handed nodes vary with the time.

Aligned MQs with a spontaneous phase synchronization (with light velocity) may also exist in an open loop, but temporally. This is a normal state of the oscillating CL node when considering the mutual interactions of the neighbouring CL nodes and this effect appears to be related to the magnetic permeability of the free space.

In a presence of charge particle, the SPM quasisphere obtains a deformation as an elongation along its diameter connecting two opposite bumps, so it is called an Electrical Quasisphere (EQ). Fig. 4 shows the shape of MQ and EQ .

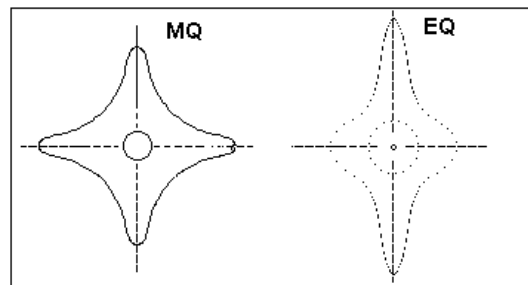


Fig. 4 Shape of MQ (left) and EQ (right)

For analysis simplification when studying the dynamics, the positions of the CL nodes could be considered as stationary in a laboratory frame. The electrical field could be presented as spatially oriented and synchronized EQ CL nodes. When studying the conditions of energy propagation as a wave, it is convenient to use imaginary *running CL nodes*. Then the phase propagation of the SPM vector with a speed of light through stationary positioned CL nodes can be regarded as a running SPM vector. In this manner, the temporal variation of the common synchronization of the CL nodes is easily studied. The analysis in such approach leads to unveiling the structure of the photon. It is found that the EQ type node possesses a larger energy than MQ type (see section 2.10.4.3 Chapter 2 of BSM). The photon wavetrain can be presented as a complex arrangement of *running EQs* with a decreasing elongation from the central axis of the wavetrain to its boundary radius, where they are converted to *running MQs*. Thus, it appears that the photon wavetrain possesses boundary conditions (a long standing problem). In the same time the running EQs are align in a helix with a step equal to the photon wavelength.

The analysis of the CL node dynamics as EQ and MQ type and the suggested photon wavetrain structure in a normal CL space (possessing a normal Zero Point Energy) are presented in Chapter 2 of BSM. The CL space

with a subnormal Zero Point Energy and the behaviour of the charge particles in such case are analysed in Chapter 4 of BSM.

The applied new approach allows admitting that the elementary particles also possess underlying structure built by the same sub-elementary particles – the two types of prisms. BSM analysis leads to a conclusion that the stable particles, such as proton, neutron and electron (and positron) possess stable structures with well-defined spatial geometry and denser internal lattices. They are comprised of complex but understandable three-dimensional helical structures whose elementary building blocks are the mentioned above prisms, arranged in a strong particular order. The analysis provided in chapter 8 of BSM leads to a conclusion that the protons and neutrons are spatially arranged in the atomic nuclei¹⁵. If the suggested vacuum structure is real, the interpretation of the scattering experiments should be reconsidered, because both, the vacuum structure and the structure of the elementary particles have not been taken into account, so far.

3. A physical model of the electron built by the suggested sub-elementary particles

According to the BSM concept, the electron possesses the simplest structure among the stable elementary particles. The suggested physical model of the electron is comprised of three helical structures, one inside another, as illustrated in Fig. 5. The helical structure is comprised of a helical envelope and internal lattice inside this envelope. All of them are built by the suggested sub-elementary particles (prisms). The axial section of an elementary core from any helix envelope contains 7 prisms of the same type, one in the centre and 6 in the periphery. In the same time they are axially displaced (as shown in Fig. 5), so the helix could be considered as formed of stacked elementary cores. The two helical structures of the electron possess denser internal lattices located in the internal spaces of the helix envelopes (not shown in this figure).

The dimensions of the physical components of the electron structure are denoted as : R_c – the Compton radius of electron (known), r_e - a small electron radius, r_p - a small positron radius, s_e – a helical step. The derivation of these dimensions is discussed later.

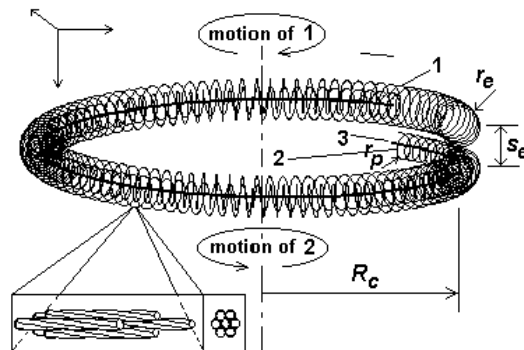


Fig. 5. Oscillating electron is comprised of three helical structures: 1 – external negative, 2 - internal positive, 3 – internal negative core. The internal lattices are not shown. The expanding box in the lower left side shows an elementary node of the helical structure 1, formed of 7 right-handed prisms (they are not externally twisted, the twisting is for a concept visualization only)

The electron structure, shown in Fig. 5 has two internal lattices spaced inside the volume enclosed by the two helical structures. Each one is built of same type of prisms like their envelopes. The outer lattice has a larger whole in its radial section where the internal first order helical structure oscillates. The other internal lattice has a smaller whole where the internal core oscillates.

The geometrical considerations allowing building of internal lattice are illustrated by Fig. 6.

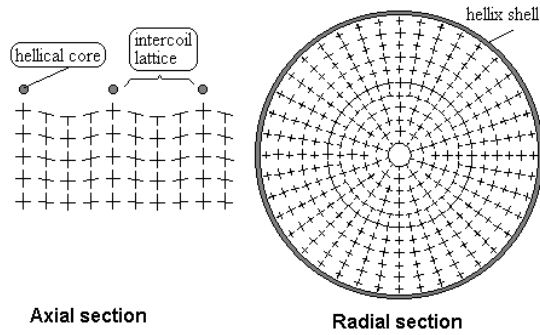


Fig. 6 Configuration of the internal lattice of type RL (Rectangular Lattice) inside the cylindrical space enveloped by the helical core, which forms the helical structure. The actual number of layers in the radial section is much larger than this shown in the figure, because the prism size is a few orders smaller than the radial section diameter

Following the geometrical considerations every RL node is comprised of rectangular arranged prisms of a same type. The question does the RL node contains 4 or 6 prisms could not be replied here, but it is not of essential importance in the presented below analysis. The axial section contains number of concentric layers. Starting from the cylindrical boundary defined by the helix envelope, the most external layer is connected to the helix by SG forces, while every internal layer is connected to the neighbouring external one. The thickness of every internal layer is half of the thickness of the neighbouring external layer. The radially aligned prisms of the neighbouring nodes are without gaps, while the gap length between the tangentially aligned prisms in the radial section varies when moving from external to the internal radius of the layer.

When considering an open formation of helical structures, as for the electron (the both ends are not connected as in a torus) the overall configuration could not be stable if the internal lattices are of rectangular type. Such formation, however, can be stabilized if the internal RL structures get some twisting.

Figure 7 illustrates the radial section of untwisted (a) and twisted (b) RL structures, referenced respectively as RL and RL(T).

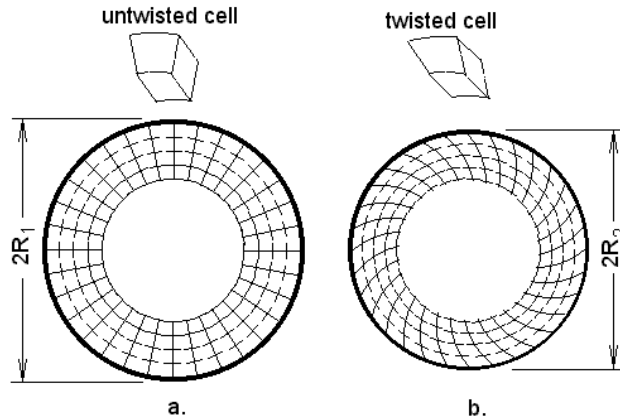


Fig. 7. Radial section of untwisted (a) and twisted (b) RL structures, referenced respectively as RL and RL(T). $R_2 < R_1$

The stiffness of the RL structure defined by the prism density is about 1000 times larger than the stiffness of the CL structure of the vacuum, so the volume of the RL structure is not penetrative even for folded CL nodes. Consequently it displaces the CL structure, or in other words, it feels a CL pressure. This is a Static CL pressure.

The twisted radial stripes of RL(T) modulate the dynamical properties of the CL nodes in the surrounding space, more accurately their SPM quasispheres. In such way, they become EQ type nodes arranged in line extensions from the twisted radial stripes of RL(T). These spatially arranged EQ nodes form the electrical field of the charge particle, in our case – the electron. This is illustrated in Fig. 8. It is evident that in a proximity range the electrical lines might be slightly curved but in a far range they appear as emerging from a point.

One from both types of the prisms (for instance the right handed) could be associated with the negative electricity while the other with the positive one, but keeping in mind that the electrical charge is a property of the CL space, related to the presence of EQs and not a property of the prism itself.

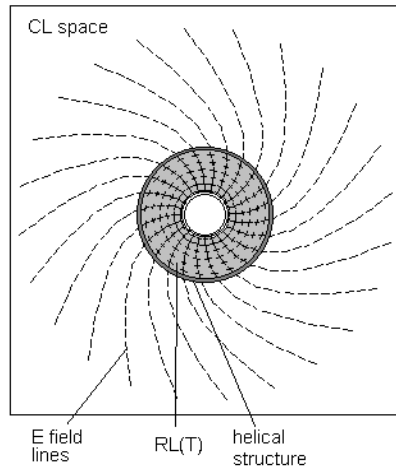


Fig. 8 Proximity E-field lines (in CL space) emerging from the RL(T) structure

The external helical structure of the electron, referenced in BSM as an external shell, possesses an internal denser lattice (from right handed prisms, for example). It is responsible for creation of EQ type CL node as radial extensions from the RL(T). The curved line extensions in the proximity to the external electron shell are of essential importance for the confined motion that the electron exhibits in CL space.

The internal helical structure with an internal RL(T) (from a left-handed prisms, respectively) with a central core (from right handed prisms) is an **internal positron**. When completely inside in the external electron shell, it is not able to modulate the external CL space, but when it is outside it appears as a positive charge. When the internal positron oscillates inside the electron external shell, its charge only partially appears in CL space with a rate of the oscillation cycle. Due to the high oscillation frequency (discussed below) only its magnetic signature may interact with the external CL space.

Considering the oscillation properties of the suggested model of the electron it could be regarded as a three-body system: an external helical structure with its internal lattice (external shell built of negative prisms), an internal helical structure with its internal lattice (internal shell built of positive prisms) and the central core (built of negative prisms). Both, the internal helical structure and the central core oscillate in conditions of ideal bearing because their central positions are kept by SG field and the whole structure has a complete helical symmetry in respect to the central core. In such conditions the electron structure will have two proper frequencies

- a first proper frequency: for the oscillations between the external electron shell and the internal positron
- a second proper frequency: for the oscillations between the internal positive shell and the central negative core (a proper frequency for the internal positron).

From the analysis of the dynamical properties of the suggested structure it appears that the first proper frequency of the electron is equal to the SPM frequency of the CL node. This is the well-known Compton frequency.

4. Quantum motion of the electron and derivation of its structural parameters

The value of the physical constants and parameters used in the presented analysis are given in Table 2 at the end of the article, before the discussions.

It is assumed and extensively discussed in BSM hypothesis that the prisms, formed of superdens intrinsic matter possess quite different inertial properties in a pure void space (the very high interaction frequency of this matter, may be closer to the Planck frequency and consequently it may have a very small inertial properties). It is apparent that the CL structure from its side possesses a time constant which is obviously defined by the proper resonance frequency of the CL node.

The analysis of the motion behaviour of the electron structure in CL space leads to a conclusion that it will possess a preferable type of a screw-like motion. Such motion in the CL space environments is possible if some CL nodes are temporally disconnected, displaced and then returned and reconnected to the CL space.

Such type of motion is referenced as a confined one. Two types of confined motion are identified: (1) a confined motion with optimal and sub-optimal velocities; (2) a confined motion with super-optimal velocities

4.1 Confined motion with optimal and sub-optimal velocities.

Both, the CL node and the rotating electron oscillate with a Compton frequency. It is found that when the tangential velocity of the rotating and oscillating electron is equal to the light velocity, the phase of its first proper frequency matches the phase of the SPM vector, propagating with a light velocity. In the same time, the internal core oscillation (with a proper frequency of three times the Compton frequency) provides a third harmonic feature for this motion. As a result the rotating and oscillating electron exhibits a maximum interaction with the CL space - a kind of quantum interaction. The electron axial velocity for this case is $V_{ax} = \alpha c$ (corresponding to a kinetic energy of 13.6 eV). It is referenced in BSM as an **optimal confined velocity** and the motion respectively as an **optimal confined motion**. We may consider that any point of the electron structure corresponding to a radius R (measured from the central point of the whole structure) moves with a tangential velocity equal to the speed of light (because it appears from the analysis that $r_e \ll R$). For such point of the structure the following relations are valid:

Peripheral velocity: c - path: $(4\pi^2 R^2 + s_e^2)^{1/2}$

Axial velocity: V_{ax} - path: s_e

Then the axial velocity is:

$$V_{ax} = cs_e / (4\pi^2 R^2 + s_e^2)^{1/2} \quad (3)$$

From the Bohr model of hydrogen we know that the kinetic energy of 13.6 eV corresponds to an electron motion in orbit of radius a_0 , with a velocity given by Eq. (4).

$$V_{ax} = (q_0^2 / 2h\epsilon_0) = \alpha c = 2.187691 \times 10^6 \text{ m/s} \quad (4)$$

where: q_0 - is the elementary charge, h - is the Planck constant, ϵ_0 - is the permittivity of the vacuum, α - is the fine structure constant and c - is the light velocity.

Therefore, we arrive to the following two conclusions:

- (1) The screw-like motion of the suggested electron model with a tangential velocity equal to the speed of light is energetically equivalent to an electron motion in a circular orbit of radius, a_0 , according to the Bohr model of the hydrogen.
- (2) The fine structure constant appears to be a ratio between the axial and tangential velocity of the electron, when it performs an optimal confined motion.

Combining Eq. (3) and (4) we obtain a step to radius ratio of the electron

$$R/s_e = (1 - \alpha^2)^{1/2} / 2\pi\alpha = 21.809 \quad (5)$$

Now let us assume that the first proper frequency of the electron is equal to the Compton frequency (a parameter of the CL node) and the electron structure makes one full rotation for time duration equal to the Compton time, t_c , that is an reciprocal to the Compton frequency.

$$path = 2\pi R = ct_c = c(1/v_c) \quad (6)$$

Solving the system of Eq. (5) and (6) we get the value of R and s_e .

$R = 3.86159 \times 10^{-13}$ (m) - the large radius of electron

$s_e = 1.77061 \times 10^{-14}$ (m) - the helical step

It is not a surprise that the obtained value for R is exactly the Compton radius R_c , which is experimentally determined by Arthur Compton. Substituting R with R_c in Eq. (5) and having in mind that $2\pi R_c = \lambda_c$, we obtain an expression for the helical step, s_e .

$$s_e = \alpha \lambda_c / (1 - \alpha^2)^{1/2} \quad (7)$$

The Compton wavelength, λ_c is related to the Compton frequency, ν_c , by the simple expression $\lambda_c = c/\nu_c$. The light velocity is related to the resonance frequency of the CL node, while the Compton frequency is the SPM frequency. Then from Eq. (7) follows a conclusion that:

The suggested model of the electron is characterised by two embedded fundamental constants: the fine structure constant and the Compton wavelength.

From number of considerations given in section 3.6 and 3.11.2 of Chapter 3 in BSM it appears that $s_e \approx 2r_e$, and it is assumed that this relation is more accurately expressed by the gyromagnetic factor, g_e , that is experimentally determined with high accuracy.

$$s_e = g_e r_e = 2.002319 r_e \quad (8)$$

From the analysis of the Fractional Quantum Hall experiments in Chapter 4 of BSM, it is found that: $r_p/r_e = 2/3$. Then all geometrical parameters of the electron are determined.

At the optimal confined motion with a velocity $V_{ax} = \alpha c$ (13.6 eV) the quantum interaction of the oscillating electron with the oscillating CL nodes are strongest. It is apparent that the electron may perform a screw-like motion also with smaller velocities. Let considering these velocities for which the electron makes a complete rotation for a whole number of first proper frequency cycles. Such set of axial velocities could be expressed by Eq. (9), where n is an integer.

$$V_{ax} = \alpha c / n \quad (9)$$

If using the kinetic energy of the electron instead of its axial velocity we have

$$E = 0.5 h \nu_c \alpha^2 / n^2 \quad (J) \quad (10)$$

$$E_{ev} = 0.5 h \nu_c \alpha^2 / (n^2 q_0) \quad eV \quad (11)$$

where: h – is the Planck constant, ν_c - is the Compton frequency, q_0 - is the electron charge

The integer n is called in BSM a **subharmonic number**, in order to notify the quantum motion conditions of the electron. A quantum motion with a first harmonic velocity corresponds to 13.6 eV, with a second subharmonic - 3.4 eV, with a third subharmonic - 1.51 eV and so on. It is evident that the introduced subharmonic number, n , matches the quantum number of the electron orbit in the Bohr atomic model. In the same time it is informative about the rotational spin motion of the oscillating electron if referencing its rotation cycle to the SPM cycle of the CL space:

13.6 eV - 1 rotation cycle per SPM cycle (an optimal confined motion)

3.4 eV - 1/2 rotation cycle per SPM cycle

1.51 eV - 1/3 rotation cycle per SPM cycle

0.85 eV = 1/4 rotation cycle per SPM cycle

SPM cycle period = Compton time

Analysing the confined motion of the electron, it is possible to get some insight about its influence on the SPM quasispheres surrounding its trace of motion. It is found that the surrounding EQs of the moving electron will cause a formation of spatially ordered synchronization of the surrounding MQs in closed loops, i. e. creation of magnetic lines. In such aspect it is useful to analyse the magnetic radius of the electron at different subharmonic numbers. We may consider that the rotating SG field of the internal lattice of the electron helical structure (that modulates the CL space) could not exceed the light velocity. Then the magnetic influence could be extended up to some limited range and we may regard it as a magnetic radius.

The magnetic radius of electron with a kinetic energy of 13.6 eV is obtained from the analysis of the quantum magnetic field Φ_0 (see section 3.11 in Chapter 3 of BSM): $\Phi_0 = h/q_0$, where h – is the Planck constant, q_0 – is the electrical charge. The obtained value of r_{mb} for 13.6 eV is almost equal to R_c , but slightly larger due to the finite thickness of the electron helical structure. The electron model gives also some insight about its magnetic moment. The magnetic moment of the electron is considered anomalous because it is distinguished from the Bohr definition of magnetic moment by the term $\alpha/(2\pi)$.

$$\mu_e = \frac{q_0 \hbar}{4\pi m_e} \left(1 + \frac{\alpha}{2\pi}\right) \quad (12)$$

where: m_e – is the mass of the electron

The anomalous term in Eq. (12) appears because the overall shape of the electron is not a torus but a single coil, possessing a helical step. Having such shape the electron is able to advance by a size of a full step, s_e , for one revolution, so these feature contributes to the “anomalous” term $\alpha/(2\pi)$. This feature is not taken into account when the magnetic moment is defined from the considerations of the Bohr atom. The magnetic moment is discussed in details in section 3.11 Chapter 3 of BSM.

4.2 An Electron motion with super-optimal velocities

The optimal confined motion of the electron (axial velocity of $V_{ax} = \alpha c = 2.18769 \times 10^6$ (m/s)) could be regarded as an ideal case of the screw-like motion. In such motion the rim of the electron structure slides like in a thread and the oscillation of the central core (with a proper frequency three times higher than the first proper frequency) provides a hummer-drill effect enhancing the interaction with the stationary CL nodes. Keeping in mind that the phase of the SPM frequency propagates with the speed of light it is evident that the screwing electron is moving as in a lubricated thread. At this quantum velocity the electron exhibits a maximum quantum interaction with the CL space. For larger velocities (or energies larger than 13.6 eV), the motion is still confined, but the screwing is not like in a thread (because no point of the electron structure could exceed the light velocity, which is restricted by the proper resonance frequency of the CL node). Therefore, we may expect a decrease in the quantum efficiency for such velocities. This is discussed in section 3.11.A.1, Chapter 3 of BSM, where an expression for the quantum efficiency is derived. The obtained expression appears to be a reciprocal function of the relativistic gamma factor. This is in agreement with the mass increase of the electron at relativistic velocities.

5. Rydberg constant as a signature of the optimal confined motion of the electron

Let considering a quantum motion of the electron (13.6 eV) with an optimal confined velocity ($n=1$, n – is a subharmonic number). The electron energy for $n=1$ according to Eq. (10) is

$$E = 0.5h\nu_c \alpha^2 \quad (J) \quad (13)$$

The energy of 13.6 eV photon is expressed by

$$E = h\nu_c = hc\sigma \quad (J) \quad (14)$$

where: $\sigma = 1/\lambda_c$ - is the wavenumber, ν_c - is the Compton frequency, c – is the light velocity

Equations (13) and (14) provide one and a same energy (13.6 eV). Solving this system for σ , we get the Rydberg constant in wavenumbers

$$\sigma = R_\infty = \frac{\nu_c \alpha^2}{2c} = 1.097373156 \times 10^7 \quad [1/m] \quad (15)$$

The suggested model of the electron contains an embedded fine structure constant as seen from Eq. (7). Additional analysis in BSM (section 2.9.6.B of Chapter 2 and section 9.7.5 of Chapter 9, from the first edition of BSM) indicates that the fine structure constant is in fact an intrinsic parameter of the CL space. The Compton frequency is also a CL space parameter characterizing the CL node dynamics. Then from Eq. (15) it follows that the Rydberg constant is also a CL space parameter. The way it was derived indicates that **the Rydberg constant appears as a characteristic feature of the quantum motion of the electron with an optimal confined velocity.**

6. Quantum motion of the electron in a closed loop trajectory.

The orbital motion of the electron in atoms could be regarded as a motion in a closed loop, whose trajectory follows the equipotential surface of an electrical field defined by one or more positive charges.

Let considering a repetitive motion in a closed loop. The modulation properties of the internal RL(T) lattice in a repetitive motion may cause distortion of the MQs (that is a normal state of the SPM vector) converting them into EQs. This will affect the orbital conditions defined by the proximity field of the proton. Let assuming that the

orbital motion of the oscillating electron tends to adjust itself to this change by exchanging some reactive energy with the CL space, that is hidden for the external observer. Then we may analyse the phase repetitions of the two proper frequencies of the electron and the conditions of their match to the phase of the SPM frequency of the CL nodes. In such way we may assume that the stability of a repetitive motion in such loop will depend on the phase repetition for both, the first and the second proper frequencies of the electron.

We will try to find the smallest path length at which the quantum loop conditions for an electron moving with a velocity corresponding to $n = 1$ (13.6 eV) is fulfilled. **Initially we will ignore the relativistic effect for simplicity.** It is reasonable to look for a path length defined by some CL space parameter. One such parameter is the Compton wavelength λ_c , related to the Compton frequency ν_c by the simple expression $\lambda_c = c/\nu_c$. For one orbital cycle in a closed loop with length λ_c , the number of turns (electron structure rotations), N_T , is:

$$N_T = \lambda_c/s_e = 137.03235 \quad (16)$$

The value of N_T could be regarded as a condition for a phase repetition for two consecutive passages through a chosen point in the loop, keeping in mind a confined (screw-like motion) of the electron. The trace length of $\lambda_c = 2.4263 \times 10^{-12}$ (m), however, is quite small, when comparing to the Bohr orbit length of $2\pi a_0 = 3.325 \times 10^{-10}$ (m). Therefore, we may look for a phase repetition conditions at larger loop length. From Eq. (16) we see that N_T is close to $1/\alpha = 137.036$ and this seems not occasional. Then, we may substitute N_T in Eq. (16) by $1/\alpha$ and multiply the result by λ_c . The latter is a CL space parameter from one side (a length of SPM phase propagation for one SPM cycle) and from the other - the circumference length of the electron structure. In such case we obtain:

$$N_T \lambda_c = \frac{1}{\alpha} \lambda_c = 3.24918460 \times 10^{-10} \quad (\text{m}) \quad (17)$$

We see that the obtained value of Eq. (17) having a dimension of length is equal to the Bohr orbit length given by CODATA 98 (see Table 2) up to the 9th significant digit.

$$2\pi a_0 = 3.24918460 \times 10^{-10} \quad (\text{m}) \quad \text{CODATA} \quad (18)$$

where: $a_0 = 0.5291772083 \times 10^{-10}$ (m) - is the radius of the Bohr atomic model of hydrogen.

The expression (17) is not something new. The important, fact, however, is the way of its derivation related with the suggested physical model of the electron. The obtained loop length appears equal to the orbit length of the Bohr atom, defined by Bohr atomic radius, a_0 . The latter is one of the basic parameters used in Quantum mechanics. From the BSM point of view, however, the physical meaning of this parameter appears different.

According to BSM concept, the well known parameter a_0 used as a radius in the Bohr model, appears defined only by the quantum motion conditions of the electron moving in a closed loop with an optimal confined velocity corresponding to an electron energy of 13.6 eV. Then the main characteristic parameter of the quantum loop is not its shape, but its length.

The identity of Eq. (17) and (18) also indicates that **the signature of the fine structure constant is embedded in the quantum loop.**

Now we may use the new obtained meaning about the quantum loop associated with the Bohr orbit, and more specifically the orbital length $2\pi a_0$. For a motion with an optimal confined velocity, the number of electron turns in the quantum orbit is equal to the orbital length divided by the helix step (s_e).

$$\frac{2\pi a_0}{s_e} = \frac{\lambda_c}{\alpha s_e} = 18778.365 \quad \text{turns} \quad (19)$$

Let find at what number of complete orbital cycles (for orbit length of $2\pi a_0$) the phase repetition of the first and second proper frequencies of the electron is satisfied (in other words the smallest number of orbital cycles containing whole number of two frequency cycles). The analysis of the confined motion of the electron in Chapter 3 and 4 of BSM indicates that its secondary proper frequency is three times higher than the first one (the first one is equal to the Compton frequency). Equation (19) shows that the residual number of first proper

frequency cycles is close to 1/3. If assuming that it is exactly 1/3 (due to a not very accurate determination of the involved physical parameters), then the condition for phase repetition of both frequency cycles will be met for three orbital cycles. The whole number of turns then should be $3\lambda_c/(\alpha s)_e$. Substituting s_e by its expression given by Eq. (7) we get

$$\frac{3(1-\alpha^2)^{1/2}}{\alpha^2} \quad (20)$$

We have ignored so far the relativistic correction, but for accurate estimation it should be taken into account. The relativistic gamma factor for the electron velocity of $V_{ax} = \alpha c$ is $\gamma = (1-\alpha^2)^{-1/2}$. Multiplying the above expression by the obtained gamma factor we get.

$$3/\alpha^2 = \text{integer} \quad (21)$$

The validity of Eq. (20) and (21) could be tested by the following simple procedure: calculating these expressions by using the best experimental value of α , rounding the result to the closer integer (satisfying the condition for two consecutive phase repetitions) and recalculating the corresponding value of α . The rounded integer (a whole number of turns) could be correct only if the recalculated value is in the range of the accuracy of the experimentally determined α . Let using the recommended value of experimentally measured α according to CODATA 98.

$$\alpha = 7.297352533(27) \times 10^{-3} \quad (\text{CODATA 98})^{16} \quad (22)$$

where, the uncertainty error is denoted by the digits in the brackets.

The calculated values of α from Eq. (20) and (21) exceeds quite a bit the uncertainty value of experimentally determined α given by Eq. (22). Consequently, the condition for phase repetitions of the two proper frequencies is not fulfilled for three orbital cycles with total trace length of $3 \times 2\pi a_0$. Therefore, we may search for the next smallest number of orbital cycles in which the phase repetition conditions are satisfied. It stands to reason that the approximate value of the orbital cycles could be about 137 ($1/\alpha$). Then if not considering relativistic correction, the corresponding number of electron turns is $(1-\alpha^2)/\alpha^3$. When applying a relativistic correction (multiplying by the estimated above gamma factor for the kinetic energy of 13.6 eV) the number of the electron turns becomes $1/\alpha^3$. The phase repetition conditions will be satisfied if this number is integer: $1/\alpha^3 = \text{integer}$

Substituting α by its value from CODATA 98 (Eq. (22)) we get $1/\alpha^3 = 2573380.57$

It is interesting to mention, that the closest integer value of 2573380 is obtained by Michael Wales, using a completely different method for analysis of the electron behaviour (See Michael Wales book "Quantum theory; Alternative perspectives")¹⁷.

We may use one additional consideration, for validation the above obtained number. The number of turns multiplied by the time for one turn (the Compton time) will give the total time on the orbit (or the lifetime of the excited state, according to the Quantum Mechanics terminology). If accepting that the total number of turns are 2573380 then we obtain a lifetime of 2.0827×10^{-14} (s), that appears to be at least two order smaller than the estimated lifetime for some excited states of the atomic hydrogen.

Following the above analysis we may check for phase repetition at $1/\alpha^4$ turns. The participation of α at power of four is in agreement also with the following consideration: In the analysis of the vibrational mode of the molecular hydrogen, an excellent match between the developed model and observed spectra (section 9.7.5 in Chapter 9 of BSM) is obtained if the fine structure constant participates at a power of four. In such case we may accept that the phase repetition conditions is satisfied for a number of turns given by the closest integer according to Eq. (23).

$$1/\alpha^4 = \text{integer} \quad (23)$$

Using the CODATA value of α we obtain $1/\alpha^4 = 352645779.39$. Rounding to the closest integer we obtain an expression for the theoretical value of α (if its experimental estimation is accurate enough).

$$\alpha = (352645779)^{-1/4} = 7.2973525298 \times 10^{-3} \quad (24)$$

The small difference of the theoretically obtained value of α from the experimental one could be caused by an experimental error. One of the methods for accurate experimental estimation of α is based on the measurement of the Josephson constant, K_J . Its connection to α is given by the expression

$$K_J = \frac{2}{c} \left(\frac{2\alpha}{\mu_0 m_e \lambda_c} \right)^{1/2} \quad (25)$$

where: μ_0 - permeability of vacuum, m_e - electron mass, c - light velocity, λ_c - Compton wavelength.

The accuracy of α according to this method depends mostly on the accuracy of the Josephson constant measurement, because all other parameters are accurately known. The recommended value for this constant according to CODATA 98 is $K_J = 483597.898(19) \times 10^9$ (Hz/V). If replacing α in Eq. (25) with the value given by Eq. (22) we will obtain the value of K_J that is in the uncertainty range given by the CODATA 98.

The conclusion that the orbital time duration may depends only on α is reinforced also by the consideration that the Compton wavelength, λ_c , was initially involved in the analysis (Eq. (15), (17), (19)), but it disappeared in the derived Eq. (23). Consequently, the phase repetition condition is satisfied not only for the two proper frequencies of the electron, but also for the SPM frequency of the CL nodes included in the quantum orbit (λ_c is the propagated with a speed of light phase of the SPM vector for one SPM cycle of the CL node (SPM frequency = Compton frequency)).

Table 1 shows the quantum motion parameters of the electron in a quantum loop for velocities corresponding to different subharmonic numbers.

Table 1. Quantum motion parameters of the electron in a quantum loop

n	E (eV)	V_{ax}	V_t	r_{mb}	l_{ql}	L_q (Å)
1	13.6	αc	c	$\sim R_c$	$2\pi a_0$	1.3626
2	3.4	$\alpha c/2$	$c/2$	$2R_c$	$2\pi a_0/2$	0.6813
3	1.51	$\alpha c/3$	$c/3$	$3R_c$	$2\pi a_0/3$	0.4542
4	0.85	$\alpha c/4$	$c/4$	$4R_c$	$2\pi a_0/4$	0.3406
5	0.544	$\alpha c/5$	$c/5$	$5R_c$	$2\pi a_0/5$	0.2725

Table notations: n - is the subharmonic number, E - is the electron energy, V_{ax} - is the axial velocity, V_t - is the tangential velocity of the rotating electron structure, r_{mb} - is the equivalent magnetic radius of the electron limited by the speed of light modulation of the CL nodes from the rotating electron structure, c - is a light velocity, R_c - is the Compton radius, a_0 - is the Bohr radius, l_{ql} - is the trace length for a motion in closed loop (single quantum loop), L_q - is the length size of a quantum loop if its shape is a Hippoped curve with a parameter $a = \sqrt{3}$ (close to the shape of digit 8).

The introduced parameter subharmonic number shows the rotational rate of the whole electron structure.

7. Quantum orbits.

It is apparent from the provided analysis that a stable quantum loop is defined by the repeatable motion of oscillating electron. The shape of such loop, however, is determined by external conditions. Such conditions may exist in the following two cases:

- a quantum loop obtained between particle with equal but opposite charges and same mass, as in the case of positronium (see Chapter 3 of BSM)
- a quantum loop obtained between opposite charged particles but with different masses (a hydrogen atom as a most simple case and other atoms and ions as more complex cases).

In both options the quantum loops are repeatable and we may call them **quantum orbits**. A single quantum orbit could contain one or few serially connected quantum loops (in both cases the condition for phases repetition is preserved). It is obvious that the shape of the quantum orbit is defined by the proximity field configuration of the proton (or protons). The vacuum space concept of BSM allows unveiling not only the electron structure but also the physical shape of the proton with its proximity electrical field (chapters 6 and 7 of BSM). The shape of any possible quantum orbit is strictly defined by the geometrical parameters of the proton.

Let considering now the induced magnetic field of the electron motion in a quantum orbit by using the electron magnetic radius. The magnetic radius of the electron moving with different subharmonic numbers n is analysed in section 3.1, Chapter 3 of BSM. Its value for $n = 1$ (a kinetic energy of 13.6 eV) matches the estimated magnetic radius corresponding to the magnetic moment of the electron. For larger numbers (decreased electron energy), however, the magnetic radius shows an increase. The physical explanation by BSM is that at decreased rate of the electron rotation its SG field of the twisted internal RL structure is able to modulate the surrounding CL space up to a larger radius until the rotating modulation of the circumference reaches the speed of light. Keeping in mind that the circumference of the electron is equal to the Compton wavelength (with a first order approximation) the circumference length of the boundary (defined by the rotation rate) should be a whole number of Compton wavelengths. Then the integer number of the Compton wavelengths corresponds to integer subharmonic number. In such case, the orbiting electron with optimal or sub-optimal velocity could not cause external magnetic field beyond some distance from the nucleus. This provides boundary conditions for the atoms, if accepting that in any quantum orbit the electron is moving with optimal or sub-optimal confined velocity (integer sub-harmonic number). Here we must open a bracket that the higher energy levels in heavier elements come not from a larger electron velocity but from the shrunk CL space affected by the accumulated protons and neutrons. Such CL space domain is pumped to larger energy levels in comparison to the CL space surrounding the hydrogen atom.

The existence of the SG law changes significantly the picture of the orbiting electron in a proximity field of the proton. In Chapter 7 of BSM an analysis of Balmer model of Hydrogen atom is developed based on the BSM concept of the electron and proton and the SG law influence on the orbital electron motion in the proximity to the proton. It appears that the limiting orbit has a length of $2\pi a_0$ while all other quantum orbits are inferior. This conclusion is valid not only for the Balmer series in Hydrogen but also for all possible quantum orbits in different atoms, if they are able to provide line spectra. Therefore, the obtained physical model of Hydrogen puts a light for solving the boundary conditions problem of the electron orbits in the atoms.

8. Time duration for a stable orbit (lifetime of excited state).

The following analysis could be valid only for the hydrogen, where the influence of the proton mass on the surrounding CL space appears to be negligible.

Keeping in mind the screw-like confined motion, the axial and tangential velocities will be inverse proportional to the subharmonic number. Then the condition for phase repetitions for a motion with a subharmonic number n will be satisfied for n times smaller number of electron turns, or the quantum orbit will be n times smaller. It is reasonable to consider that the first and second proper frequencies of the electron are stable and not dependant on the subharmonic numbers. Then for estimation of the time duration of the orbit (the lifetime of excited state) it is more convenient to use the number of the cycles of the first proper frequency of the electron. It is equal to the number of electron turns for $n = 1$. In such way we arrive to the conclusion:

- (a) If conditions for stable quantum orbit are defined only by the phase repetition conditions and the whole number of Compton wavelengths, the time duration (lifetime) of the orbiting electron does not depend on the subharmonic number of its motion.
- (b) If (a) is valid, the lifetime of the excited state will be equal to the product of the total number of the first proper frequency electron cycles (according to Eq. (23)) and the Compton time (the time for one electron cycle with the first proper frequency)

According to condition (b) the theoretical lifetime for an excited state of hydrogen is

$$\tau = t_c / \alpha^4 = \lambda_c / (c\alpha^4) = 2.85407 \times 10^{-12} \text{ (s)} \quad (26)$$

where: t_c - is the Compton time.

Note: The obtained Eq. (26) does not take into account the possible modification of the surrounding space in a close proximity to the proton. Such modification (a slight shrinkage, or a space curvature) may cause aliasing for the phase repetition conditions due to affected SPM frequency and Compton wavelength, while the first and second proper frequencies of the electron are obviously stable. For heavier atoms such modification may appear much stronger. For elements with more than one electron the mutual orbital interactions also may lead to increase of the real lifetime.

The physical constants used in this article are given in Table 2.

Table 2. Used fundamental constants¹⁶ according to CODATA 98

Constants	Value	Unit	Name
α	$7.297352533(27)\times 10^{-3}$		fine structure constant
c	2.99792458×10^8	m/s	light velocity
λ_c	$2.426310215\times 10^{-12}$	m	Compton wavelength
h	$6.62606876(52)\times 10^{-34}$	Js	Planck constant
ϵ_0	$8.854187817\times 10^{-12}$	F/m	permittivity of free space
m_e	$9.10938188(72)\times 10^{-31}$	kg	electron mass
a_0	$0.5291772083(19)\times 10^{-10}$	m	Bohr radius
K_J	$483597.898(19)\times 10^9$	Hz/V	Josephson constant
R_∞	$1.973731568549(83)\times 10^7$	1/m	Rydberg constant

9. Conclusions and comments

According to the BSM hypothesis, the physical model of the electron possesses a structure built by sub-elementary particles, which are also involved in the underlying hypothetical structure of the space (the physical vacuum). The suggested electron model with a signature of anomalous magnetic moment exhibits rich oscillation and interaction behaviour in such space. Two fundamental physical constants as the fine structure constant and the Compton frequency (or wavelength) appear embedded in the electron structure and its dynamical behaviour. The analysis leads to the conclusion that the Compton frequency, ν_c , expresses simultaneously two different features: the SPM frequency of the CL node and the first proper frequency of the oscillating electron. At the same time, the Compton wavelength, λ_c , expresses the length of the phase propagation of the SPM vector with a light velocity for one cycle of the SPM frequency of the CL node. This is in agreement with the relation $\lambda_c = c/\nu_c$. More details about the use of the suggested electron structure for unveiling the meaning of different physical constants are provided in the BSM hypothesis¹³. Further analysis, presented in BSM, leads to derivation of a hydrogen model possessing boundary conditions for the electronic orbits, while exhibiting the same energy levels like the Bohr atomic model. The obtained model of the hydrogen further served as a base for the suggested spatial arrangement of the protons and neutrons in the atomic nuclei¹⁵.

10. Acknowledgements

I wish to express my gratitude to Mark Poringa for the useful comments and discussions related to the BSM hypothesis and particularly this monograph. Special appreciations and thanks are extended to acad. Prof. Dr. Asparuh Petrakiev of the Burgas University, Bulgaria, for the organized workshop in August 2003, Varvara, Bulgaria and to Angel Manev of the STIL at the Bulgarian Academy of Sciences for the useful discussions.

References:

1. L. Ferrarese, D. Merrit, A fundamental relation between supermassive black holes and their host galaxies, <http://arxiv.org/abs/astro-ph> No. 0006053 v. 2 9 Aug 2000

2. D. F. Roscoe, An analysis of 900 optical rotation curves: Dark matter in a corner?, *Phahama - journal of physics*, Indian Academy of Sciences, Vol. **53**, No 6, Dec 1999, p. 1033-1037
3. T. H. Boyer, The Classical Vacuum, *Scientific American*, Aug. 1985, p.70-78.
4. H. E. Puthoff, Gravity as a zero-point-fluctuation force, *Phys. Rev. A*, vol. 39, no 5, 2333-2342, (1989)
5. H. E. Puthoff, Polarizable-Vacuum (PV) Approach to General Relativity, *Foundations of Physics*, V. 32, No. 6, 927-943 (2002)
6. H. E. Puthoff, Can the Vacuum be Engineered for Spaceflight applications, NASA Breakthrough Propulsion Physics, conference at Lewis Res. Center, (1977)
7. H. E. Puthoff, S. Tittle, M. Ibison, Engineering the Zero-Point Field and Polarizable Vacuum for Interstellar Flight, First International Workshop in Field Propulsion, Univ. of Sussex, Brighton, UK, Jan 2001, <http://www.nidsci.org/article3.html>
8. B. Haisch, A. Rueda and H. E. Puthoff, Inertia as a Zero-point field lorentz force, *Phys. Rev. A*, **49**, 678 (1994). See also *Science* 263, 612 (1994)
9. F. M. Meno, A Planck-length Atomic Kinetic Model of Physical Reality, *Physics Essays*, **4**, p.94, (1991)
10. M. L. Gershteyn, L. Gershteyn, A. Gershteyn, O. Karagioz, Experimental evidence that the gravitational constant varies with orientation, (2002), <http://arxiv.org/abs/physics/0202058>
11. M. Ibison, H. E. Puthoff and S. R. Little. The Speed of Gravity Revisited, posted to LANL archives, <http://xxx.lanl.gov/abs/physics/9910050>
12. S. Sarg, New approach for building of unified theory about the Universe and some results, <http://lanl.arxiv.org/abs/physics/0205052>
13. S. Sarg, "Basic Structures of Matter", monograph, (2001), <http://www.helical-structures.org> also in National Library of Canada, (2002) <http://www.nlc-bnc.ca/amicus/index-e.html> (AMICUS No. 27105955) (first edition)
14. S. Sarg, Brief introduction to the Basic Structures of Matter Theory and derived atomic models, *Journal of Theoretics*, (2003), www.journaloftheoretics.com/Links/Papers/Sarg.pdf
15. S. Sarg, Atlas of atomic nuclear structures according to the Basic Structures of Matter theory www.journaloftheoretics.com/Links?papers/Sarg2.pdf also in National Library of Canada, (2002) <http://www.nlc-bnc.ca/amicus/index-e.html> (AMICUS No. 27106037)
16. P. J. Mohr and B. N. Taylor, CODATA recommended values of the fundamental constants: 1998, *Rev. Mod. Phys.*, **72**, 351-495, (2000)
17. M. Wales, *Quantum Theory; Alternative Perspectives*, Shields Books, <http://www.fervor.demon.co.uk>